

COMPARISON STUDY BETWEEN THREE AXIS VIEWS OF VISION, MOTOR AND PRE-FRONTAL BRAIN ACTIVITIES

Marwa MohamedSheet AL-Hatab^{1,2}, Raid Rafi Omar Al-Nima², Iliaria Marcantoni¹, Camillo Porcaro^{1,3,4,5,6} and Laura Burattini¹

¹Department of Information Engineering, Università Politecnica delle Marche, Ancona, Italy

²Technical Engineering College / Northern Technical University / Iraq

³Institute of Cognitive Sciences and Technologies (ISTC) - National Research Council (CNR), Rome, Italy

⁴S. Anna Institute and Research in Advanced Neurorehabilitation (RAN), Crotone, Italy

⁵Research Center for Motor Control and Neuroplasticity, KU Leuven, Leuven, Belgium

⁶Centre for Human Brain Health, School of Psychology, University of Birmingham, Birmingham, United Kingdom

marwahatab7@gmail.com, raidrafi3@ntu.edu.iq, i.marcantoni@pm.univpm.it, camillo.porcaro@afar.it, l.burattini@staff.univpm.it

Abstract:The brain is the main controller of the vital processes and functional studies. The Functional Magnetic Resonance Imaging (fMRI) can provide useful indications to explain the functional activities of brain. Especially with utilizing the three image views of X_axis (Sagittal Plane) split the brain into left and right segment, Y_axis (Coronal plane) split the brain into back and front segment and Z_axis (Axial plane) split the brain into top and down segment. In this study, we propose various deep learning models namely the X_axis Classification Model (XCM), Y_axis Classification Model (YCM) and Z_axis Classification Model (ZCM) for classify three tasks of vision, movement and pre-frontal brain activities. In addition of presenting comparisons between different network models for all of the three views. After extensive experiments and comparisons even with state-of-the-art studies, promising accuracies of 91.67%, 89.88% and 91.67% have successfully been obtained for the XCM, YCM and ZCM, respectively.

Keywords:Brain Activities, Classification, Deep Learning and fMRI images

I. INTRODUCTION

fMRI is an imaging technology that is primarily used to perform brain activation studies by measuring the dependent signal of blood oxygen level. It serves as indicators for neural activities of brain [1] [2] [3]. In general, Classifying multiple categories has attracted significant attentions as in [4] [5] [6] and have been successfully applied to fMRI experiments on visual [7] [8] [9] [10], movement/motor [11] and forward/anterior activity [12] [13] tasks. These essential three tasks can be determined from the activities of specific brain parts. Firstly, the movement/motor frontal cortex part refers to performing regulated movements. It does not specify the type of movement. Classically, the motor cortex is the area of frontal lobe that is located in the posterior precentral- gyrus immediately anterior to the central sulcus [11]. Secondly, the visual cortex of the brain is that part of the cerebral cortex where the activities of visual information processes are mentioned. It is located in the occipital lobe. The optic nerves directly work from the eye to the primary visual cortex moving on to the visual cortex [14]. Thirdly, pre-frontal brain segment refers to the forward/anterior activity. The anterior part of the brain is one of three poles (along with the occipital pole and temporal pole). This part of the activity is associated with attention, short-term memory, planning and motivation tasks [15].

Several studies were considered for classifying brain activities based on the deep learning techniques. Previous studies that are related to this work are reviewed. In 2015, Suhaimi *et al.* presented a study for classifying fMRI images by exploiting the deep learning technique. Comparisons were here established for three cases based on the deep learning. These are the classification of ADHD, memory encoding, memory decoding and brain parcellation. It also seems that the Z-axis view images were utilized [16]. In 2017, Meszlényi *et al.* proposed a Connectome-Convolutional Neural Network (CCNN). This network can recognize the resting state from the fMRI images. Only the Z_axis view was employed in this work [17]. In 2018, Wen *et al.* investigated deep learning methods to process the fMRI data. The application of this study was performed for diagnosing the cognitive impairment. It seems that the Z-axis views were exploited [18]. At the same year, Pallareset *al.* suggested set of new standard fMRI data for extracting the multivariate signatures. The authors recognized between different subjects of individuals. The authors also classified between the various behavioral conditions. This work was organized into two parts. Firstly, using coupled whole-brain Effective Connectivity (EC) estimation with adequate machine learning tools to control the session-to-session variability.

Consequently, comparing between the EC and Functional Connectivity (FC) is utilized as the generalization capabilities for unseeded data in order to classify single resting-state fMRI sessions with respect to (healthy) subjects. Secondly, both subjects of identity and condition (rest versus movie views) were predicted to verify that EC can disentangle the two types of signatures. Just the Z_axis views were used [19]. In 2019, VanRullen et al. applied a recently developed deep learning system to reconstruct face images from the fMRI of individuals. A Variational Auto-Encoder (VAE) neural network was trained by using a Generative Adversarial Network (GAN). Unsupervised procedure was considered over large number of celebrity faces. The results showed that some advantages of face recognition and gender classification could be taken from the expressive power of deep generative neural networks (in particular the VAEs coupled with the GANs). This led to provide better image spaces of decoded brain information. Front parietal, temporal and occipital views were considered [20]. It can be investigated that classifying the vision, movement and forward brain activities based on the three views of (X_axis, Y_axis and Z_axis) has not been considered before. Therefore, this study will be presented to overcome the obstacles of this issue.

This study is aiming to compare between the three axis views of X_axis, Y_axis and Z_axis for the vision, motor and prefrontal brain activities. The objectives and contributions of this work can be highlighted as follows:

- a) Collecting fMRI images and analyzing them based on the hypothesis of linear correlations between the neurons activities and their tasks by employing the Statistical Parametric Mapping (SPM) toolbox [21] [22]. The SPM results are obtained by the Group Ica of fMRI Toolbox (GIFT) which exploits for transferring data from statistical analyzes to the Independent Component Analysis (ICA). The goal of the ICA is de-noising signals, removing artifacts, and separating and extracting required information [23] [24].
- b) Designing and evaluating efficient deep learning networks called the XCM, YCM and ZCM for the three axes views of X_axis, Y_axis and Z_axis, respectively. Each of these models is able to classify between the vision, movement and forward brain activities.
- c) Establishing justifiable comparisons between different deep learning network models including state-of-the-art studies.

II. METHODOLOGY AND MATERIALS

1. Database

In this work, we have used an Functional Magnetic Resonance Imaging (fMRI) dataset approved by the Ethics Committee of Aston University (ECAU). The data are collected based on Event-related fMRI (efMRI) [25]. The task implemented stimulates brain regions from vision, decision making and motor. 13 Italian volunteers were enrolled for the study. All volunteers are Italian speakers, of ages between 25 – 42 years. Six of them are women. The fMRI images were acquired using 8-channels of radiofrequency head coil. Type Siemens medical systems from Germany with a 3 Tesla using Siemens Trio MRI scanner is employed. Each image was captured with the following specifications: Time of Echo (TE) equal to 30 ms, Time of Repetition (TR) equal to 3.0 s, image matrix equal to 64×64 pixels, Field of View (FOV) equal to $216 \times 216 \times 129$ mm³, flip angle equal to 90 degree, voxel size equal to 3×3 mm and slice thickness equal to 3 mm. Brain volumes were acquired in a series of slices, where a total number of slices are 44. Between 765 and 800 volumes per participant were collected in a single session [25] [26].

fMRI data were pre-processed using SPM12 (Wellcome Department of Imaging Neuroscience, London; <http://www.fil.ion.ucl.ac.uk>) and analysed by Group ICA of fMRI Toolbox (GIFT - <http://trendscenter.org/software/gift/>).

2. Classification Models

In this study, classifying various essential brain activities of motor, vision and prefrontal was designed and compared. Three views of fMRI images were employed, these are the X_axis (sagittal plane), Y_axis (coronal plane) and Z_axis (axial plane). It was investigated that increasing the viewing information of brain activities can lead to achieve better performance. For that, three deep learning models are designed and implemented to achieve high classification accuracies.

Fundamentally, this work is involved many processing stages. Firstly, collecting the fMRI images of vision, movement and prefrontal brain cortices activities by using the SPM to apply the spatial pre-processing, temporal pre-processing and statistical analyses. Then, utilizing the GIFT to identify the brain activity areas in each image. As mentioned, comprehensive study was provided by exploiting the orthogonal presentations of (X_axis, Y_axis and Z_axis). Secondly, preparing all the employed images by applying the pre-processing of cropping. Moreover, the images will be partitioned into two phases: training and testing. Thirdly, proposing three deep learning networks, each for a specific view. These are the XCM, YCM and ZCM. Fig. 1 shows the most important stages of this work.

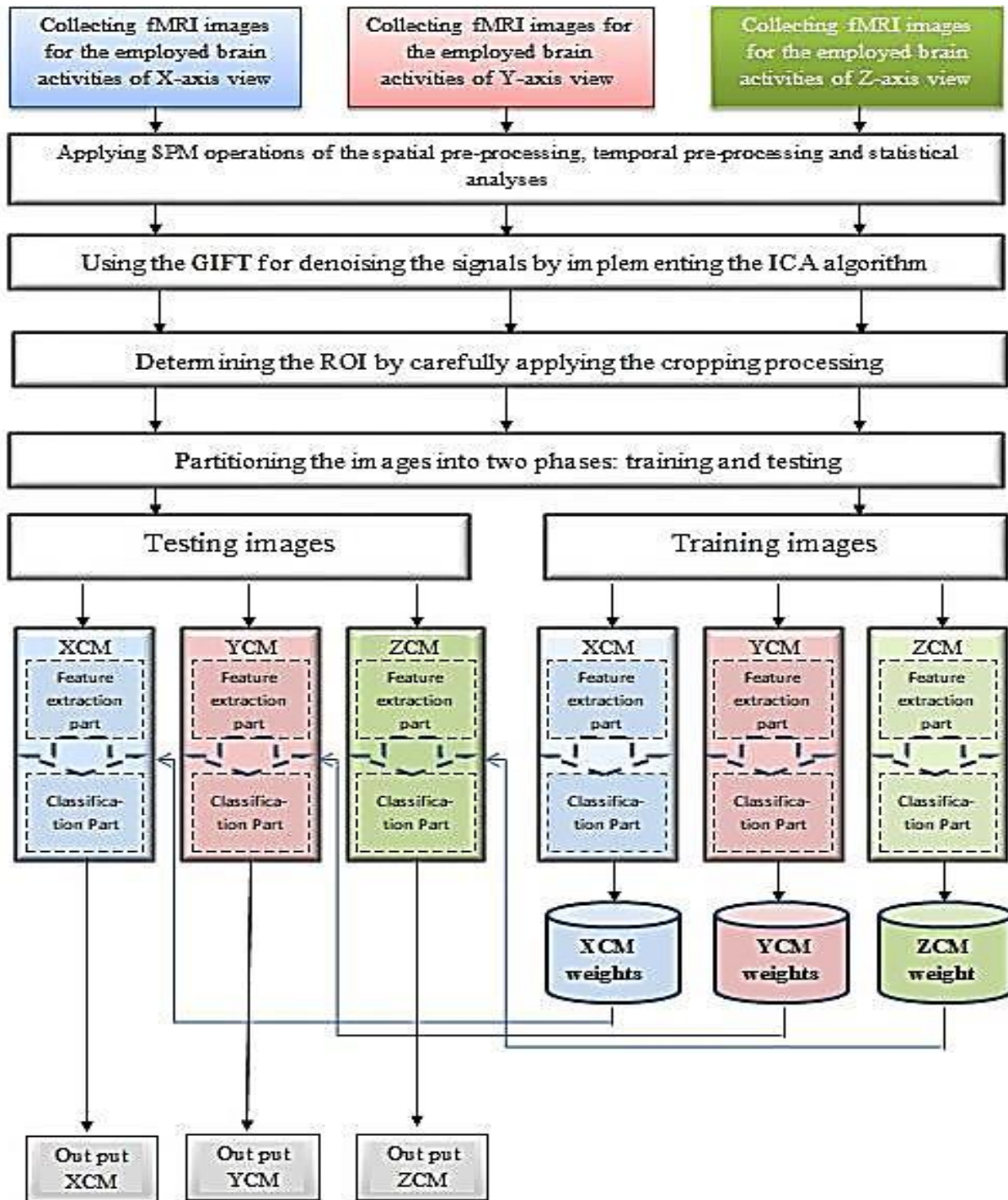


Figure 1: Required processing stages in this study

Various deep learning models XCM, YCM and ZCM are designed based on the Convolutional Neural Network (CNN). Each one of them is consisted of the following essential layers:

- ❖ Input layer deals with images. It collects values of input matrix pixels depending on the resolution and size of the image. In this study, a Joint Photographic Group (JPG) colored image with the dimensions of (width × height × 3) pixels are used. The 3 refers to three channels of Red, Green and Blue (RGB) that compose the colored image which is known as the RGB image too[27].
- ❖ Convolution layer consists of sets of image channels and kernels. In this layer, each input channel is convolved by kernels. Implementing this operation with different kernels will produce a set of feature maps.

Each kernel represents a group of weights[28].The resulted image channels known as feature maps. The feature map values are calculated according to the following formula[29]:

$$F_{u,v,c}^l = U_c^l + \sum_{i=-H_h^l}^{H_h^l} \sum_{j=-H_w^l}^{H_w^l} \sum_{c^{l-1}=1}^{c^{l-1}} W_{i+H_h^l,j,H_w^l,c^{l-1}}^{c^l} F_{u+i,v+j,c^{l-1}}^{l-1} \tag{1}$$

where: $F_{u,v,c}^l$ is an output of the convolution layer,(u,v) is a pixel coordinate, U_c^l is the channel bias, $W_{i,j,c^{l-1}}^{c^l}$ is the kernel weights, c is the channel number, H_w^l and H_h^l are respectively the width and height of the convolution layer kernel, l is the current layer, and $l-1$ is the previous layer.

❖ Rectified Linear Unit (ReLU) is the most commonly used activation function in the deep learning networks, especially in the CNN models. It works by activating an ANN to pass a positive value or zero. When comparing this with a Biological Neural Network (BNN) of brain, the activation function decides whether a neuron is fired or not [30]. It can be expressed as:

$$R_{u,v,c}^l = \max(0, F_{u,v,c}^l) \tag{2}$$

where: $R_{u,v,c}^l$ is the output of ReLU, max is the maximum operation and $F_{u,v,c}^l$ is an input positive value to the ReLU activation function[31].

❖ Pooling is down-sampling information. This layer can further reduce the spatial dimensions, but not depth. In this study, use Maximum Pooling (MP), it calculates the maximum values of small matrices (windows) in each previous feature map. The MP operation is applied according to the following equation[32]:

$$T_{a^l,b^l,c}^{Max} = \text{MAX}_{0 \leq a < p_h, 0 \leq b < p_w} R_{a^l \times p_h + a, b^l \times p_w + b, c} \tag{3}$$

where: $T_{a^l,b^l,c}^{Max}$ is an output of the pooling layer of maximum type, $0 \leq a^l < p_h^l$, p_h^l is the height of the pooled channel, $0 \leq b^l < p_w^l$, p_w^l is the width the pooled channel, $0 \leq c < c^l = c^{l-1}$, p_h is the height of each pooled window and p_w is the width of each pooled window.

❖ The fully connected (FC) layer connects each node from a previous layer to all node of this layer. It can adapt between the number of nodes in the feature extraction part and the number of nodes in the classification part of a deep learning model [33]. The output of this layer will be composed according to the following equation:

$$P_r = \sum_{a=1}^{n_1^{l-1}} \sum_{b=1}^{n_2^{l-1}} \sum_{c=1}^{n_3^{l-1}} U_{a,b,c,r}^l (T_s)_{a,b} \quad \forall 1 \leq r \leq n^l \tag{4}$$

where: P_r is an output of the FC layer, n_1^{l-1} is the previous pooling channel width, n_2^{l-1} is the previous pooling channel height, n_3^{l-1} is the number of previous pooling channels, $(T_s)_{a,b}$ is a pooling layer output, $U_{a,b,c,r}^l$ is a weight between the pooling and FC layers and n^l is the required number of classes.

❖ The softmax layer is normally applied just before the last layer, which is the classification layer. The reason of using the softmax is to provide the relating probability distributions with all output classes for a current input. However, it may become costly if the number of classes is further increased [34].Mathematically, the softmax function is shown as given in the following equation:

$$y_r = \frac{\exp(P_r)}{\sum_{s=1}^{l-1} \exp(P_s)} \tag{5}$$

where: y_r is an output of the softmax layer. In other words, the softmax function normalizes the output values of each single node to be between 0 and 1. It divides the value of each output by the total summation of other output values.

❖ The classification layer is the last layer. It classifies a provided input to its closest class. It produces the output decision. This layer operates according to the rule called the winner-takes-all [4]. The operation of this layer can be described as follows:

$$D_r = \begin{cases} 1 & \text{if } y_r = \max \\ 0 & \text{otherwise} \end{cases} \quad (6)$$

where: D_r is an output decision of the classification layer and \max represents the extracted maximum y_r value. This last layer has been adapted to classify between the motor, vision and pre-frontal brain parts depending on the location of activity. This is applied to all models of XCM, YCM and ZCM. This trend indicates that this study can reasonably succeed in providing valuable recognition of various employed brain activities for each axis.

III. RESULTS AND DISCUSSIONS

1. SPM Analyses

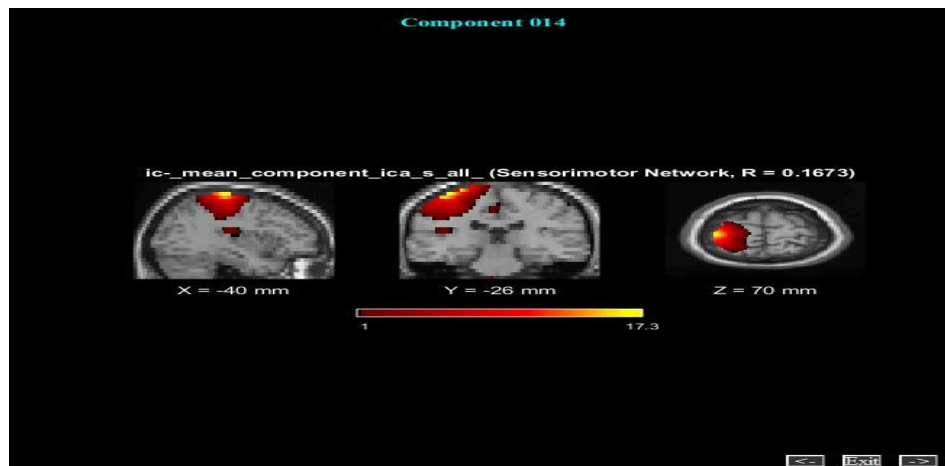
fMRI data are firstly analyzed using the SPM toolbox, where pre-processing operations are required to reduce the noise and modify the size of the fMRI data. The SPM operations include the following processes: pre-processing and statistical functions. Pre-processing functions they are divided in to temporal pre-processing and spatial pre-processing.

- Temporal pre-processing: includes the slice timing correction.
- Spatial pre-processing: includes realignment, co-registration, segmentation, normalization and smoothing.

Different techniques of image and signal processing are employed in the pre-processing steps in order to facilitate the detection, baseline correction, movement correction, image restoration, noise reduction, signal quality improvement and size modification of the fMRI data. Statistical functions: they involve the 1st-level, multiple regressions and basic functions (for modeling how the Blood Oxygen Level Dependent (BOLD) responses to neurons activity) to obtained the designed matrix which will be used in the post-processing of the GIFT toolbox.

2. GIFT Analyses

The post-processing of the GIFT toolbox, utilizing ICA allows to extract unknown source signals from known signals. It involves the following processes: ICA setup (it is for inputting the required parameters to the ICA analysis), Run analysis (it is for performing the ICA group), Analysis info (it contains all the parameters information and output files). From these processes three views of X-axis, Y-axis and Z-axis are available for the three brain activities of vision, movement and pre-front. In this work, total of 201 images which contain all the views of the three employed brain activities are extracted from 67 fMRI slices. Each slice is of size $654 \times 654 \times 3$ pixels, it is of Joint Photographic Experts Group (JPEG) format and it has a group of colored images. This data is for 13 subjects following [25][26] as to the best of the obtained knowledge full of required information are only available for those participants. Samples of brain activity slices are given in Fig. 2.



(a)

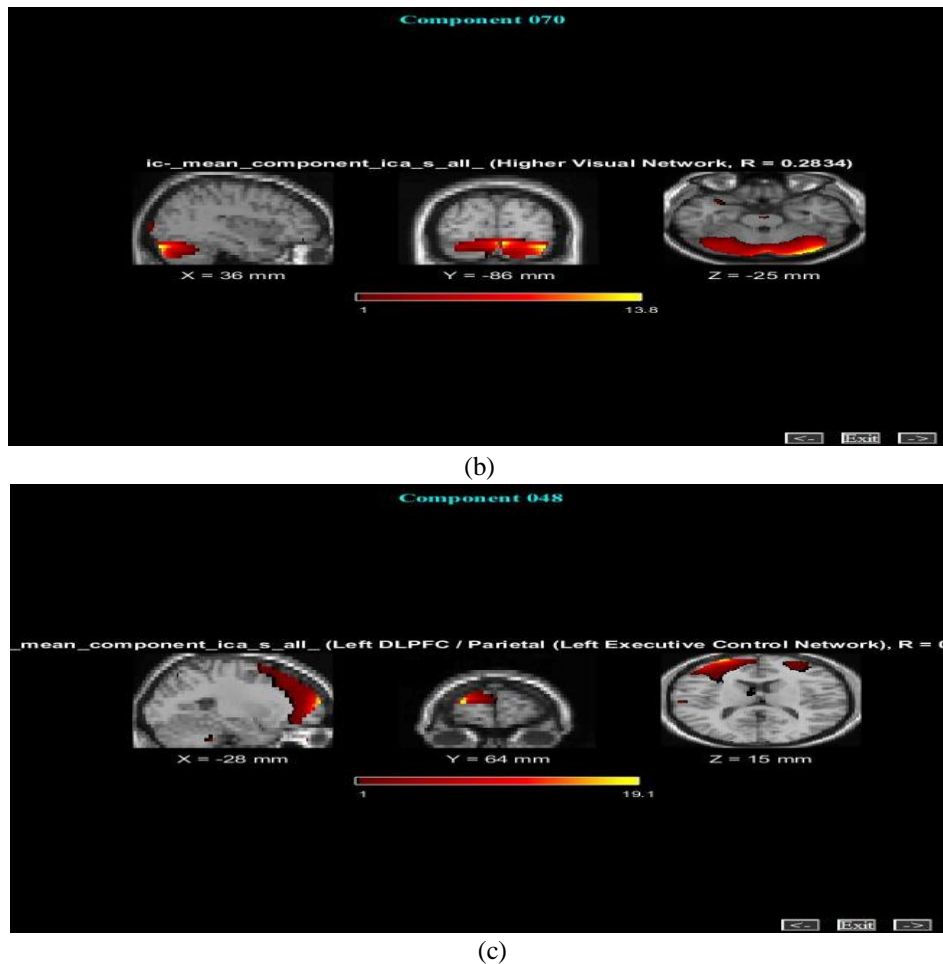


Figure 2: Samples of fMRI slices for the brain activities of motor/movement, (b) vision and (c) prefrontal. Each activity has been demonstrated from the left to the right with the views of X-axis, Y-axis and Z-axis, respectively

3. Preparing Real Clinical Data

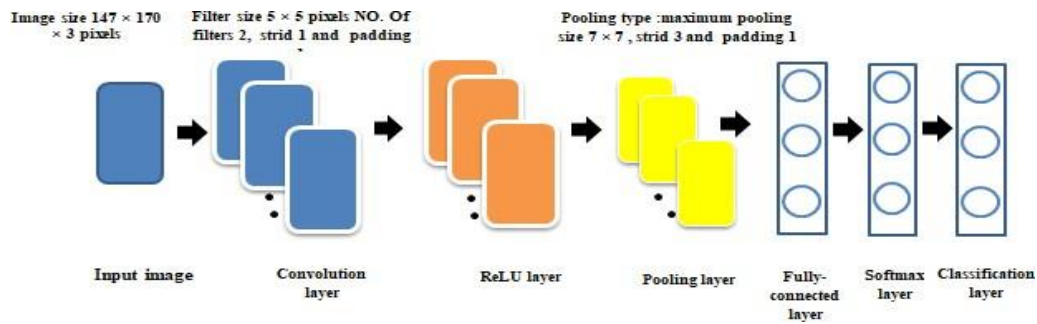
Preparing images that are obtained after previous processing is required. The applied pre-processing preparation before the deep learning classification is the image cropping. After the pre-processing, specific sizes are empirically defined for the three viewers of X, Y and Z axes. That is, a size of $147 \times 170 \times 3$ pixels is determined for the X-axis view, a size of $147 \times 140 \times 3$ pixels is assigned for the Y-axis view and a size of $147 \times 155 \times 3$ pixels is specified for the Z-axis view. Moreover, the extracted images are grouped into two phases: training and testing. In this work, all images of the employed brain activities are grouped into 50% for the training phase and 50% for the testing phase.

4. Comparisons between Proposed Deep Learning Models

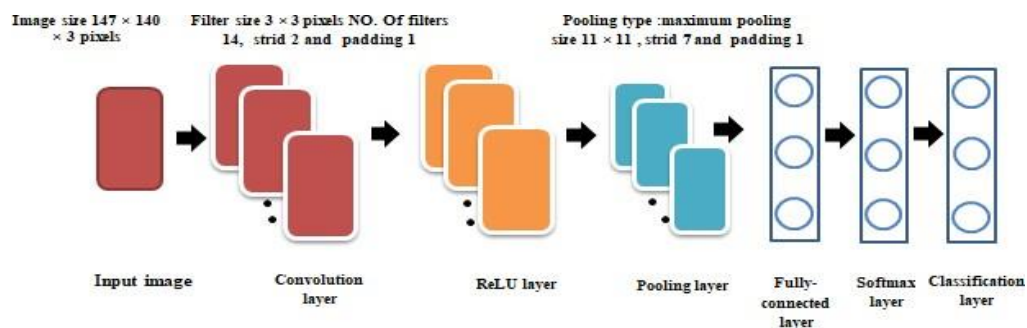
The designed deep learning models have the capability to automatically detect the important features without any human supervision. In addition, they can provide intelligent decisions or classifications.

Firstly, all the network models of XCM, YCM and ZCM are trained by utilizing the trained images set and the same networks are tested by using the tested images set. Furthermore, deep learning parameters of convolution, ReLU and pooling layers are evaluated in terms of obtaining the highest accuracies. The accuracies of each deep learning network are assessed by examining the parameters of its layers. The suggested models networks are designed, trained and tested by using a computer that has the following specifications: laptop of type Dell, Central Processing Unit (CPU) of type Intel Core (TM) i7, 3 GHz and Random-Access Memory (RAM) of 8 GB. All implementations are carried out based on the CPU.

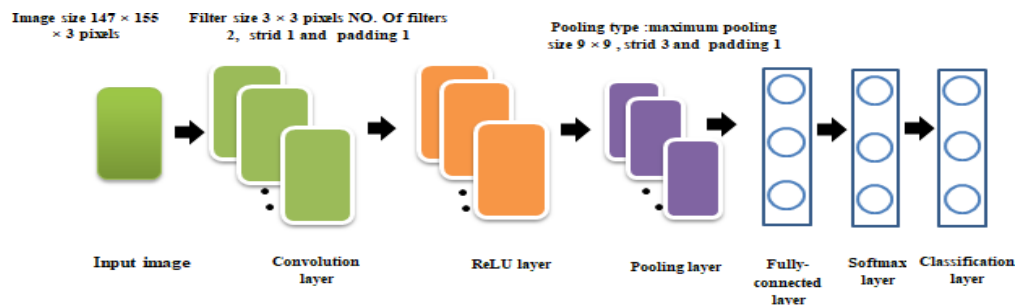
Each model of XCM, YCM and ZCM adapts to accept a specific view of fMRI images, contains evaluated parameters of its multiple layers and efficiently classifies the employed brain activities. All proposed models parameters are empirically obtained after Extensive experiments. The three models with their employed parameters are shown in Fig. 3.



(a)



(b)



(c)

Figure 3: A general architecture of the (a) XCM, (b) YCM and (c) ZCM





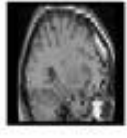








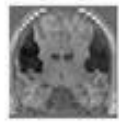






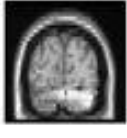









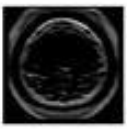



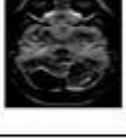

5. Comparison of Feature Extractions

In general, each one of the XCM, YCM and ZCM can be considered as a combination between two main parts: feature extraction and classification. The convolution, ReLU and pooling layers perform the feature extractions. Whilst, the FC, softmax and classification layers guide the classification. The feature extraction layers effectively and automatically acquire the patterns of motor, vision and prefrontal cortex activities as follows:

- Convolution layer: it is the first step in the feature extraction part. It applies various convolution filters on the input data and generates feature maps.
- ReLU layer: it is a nonlinear activation function. The feature extraction of the ReLU considers all the positive values of feature maps. It can detect small texture details and the resulted images will be easier to analyze.
- Pooling layer: it is to extract the most representative features of feature maps. It also reduces the size of resulted vectors.

It is a very important part because it collects the significant and presence information of previous feature maps in patches [35]. In Table 1 shows feature extractions of the XCM, YCM and ZCM in their feature extraction parts.

Table 1: Examples of feature extractions from the convolution, ReLU and pooling layers in XCM, YCM and ZCM networks

	Brain activities	Training images samples	Feature extractions of a convolution layer	Feature extractions of a ReLU layer	Feature extractions of a pooling layer
XCM	Motor activity patterns				
	Pre-frontal activity patterns				
	Vision activity patterns				
YCM	Motor activity patterns				
	Pre-frontal activity patterns				
	Vision activity patterns				
ZCM	Motor activity patterns				
	Pre-frontal activity patterns				
	Vision activity patterns				

From this table, it is possible to observe the steps of the feature extraction part for the XCM, YCM and ZCM. Patterns from the images of activated brain regions are shown, specifically for the motor, pre-frontal and vision. First appearances of patterns are provided for samples of images. In the second step, the features are extracted by the convolution layer. The automatic generated kernel values are important here as they act as feature extractors. Third step demonstrates the positive features of patterns by the ReLU layer. This step is important because a limited number of neurons are activated, which makes the network sparse, fast and has simple in computations [36]. The last step in the feature extraction part is the pooling process. The pooling layer here is of type Max. It further decreases the size of resulted vectors. So, its objective is to down-sample the representation of feature extraction vectors and preserving the essential patterns.

6. Comparisons with Other Deep Learning Models

Comparisons with different deep learning network models are implemented including state-of-the-art studies. Various network models are simulated and used for the employed database. These are the VGG-16 model [37], AlexNet model [38], Deep Finger Texture Learning (DFTL) [39], Convolutional Neural Network and Particle Swarm Optimization (CNN-PSO) [40], Extreme Learning Machine Local Receptive Fields (ELM-LRF) [41], LeNet-5 [42], faster Region-based Convolutional Neural Networks (R-CNN) [43] and Hierarchical Convolutional Neural Network (HCNN) [44]. Table 2 shows results of the applied comparisons.

Table 2: Comparisons between various deep learning network models

Approaches	Accuracy with X_axis (%)	Accuracy with Y_axis (%)	Accuracy with Z_axis (%)
VGG-16 [37]	33.33	36.11	36.11
AlexNet [38]	33.33	36.11	33.33
DFTL [39]	77.76	72.22	77.76
CNN-PSO [40]	72.22	77.78	77.78
ELM-LRF [41]	77.76	72.22	83.33
LeNet-5 [42]	72.22	75	86.11
R-CNN [43]	80.56	80.56	75
HCNN [44]	77.78	83.33	86.11
Proposed network models	91.67	88.89	91.67

The comparisons in this table are reasonable. The depth of a network in both the VGG-16 and AlexNet proved its negative effect in extracting the features of applied brain activities, adding more layers (stack of layers) leads to get high training error. They resulted in very low accuracies and recorded values of 33.33% or 36.11% for the three employed views. In addition of spending long training times. The networks DFTL, CNN-PSO, ELM-LRF, LeNet-5, R-CNN and HCNN are characterized by specific layers with different parameters. So, they have the capability to discover some features of brain activities and raise the results comparing to the VGG-16 and AlexNet. They reported different performances from a minimum value of 72.22% to a maximum value of 86.11% for the three views (X_axis, Y_axis and Z_axis). The suggested XCM, YCM and ZCM surpassed other networks including state-of-the-art models and they attained superior performances of 91.67% for the X_axis, 88.89% for the Y_axis and for the Z_axis 91.67%. They can well discover the features of employed brain activities and achieve the highest accuracies for all of the employed views.

The X_axis and Z_axis views for the fMRI images are preferable in classification studies of brain activities. This is because of the clarity of provided information. Especially the Z_axis as it can be considered as the optimal visualization view. Because the ZCM model could achieve the highest accuracy in short time. On the other hand, the Y_axis view can be considered as challenging perspective to detect brain activities. This is due to the narrow information of activities in the closest brain parts.

In summary, the proposed DL networks can be signified with other artificial intelligence models as in [45-55]. They can be utilized for important matters as [56-61].

IV. CONCLUSION

This study involved many processing stages starting from collecting the fMRI images of vision, movement and prefrontal brain cortices activities by using the SPM to apply the spatial pre-processing, temporal pre-processing and statistical analyses. Then, utilizing the GIFT to identify the brain activity areas in each image. Proposing three deep learning networks, each for a specific view. These are the XCM, YCM and ZCM.

They surpassed other state-of-the-art network models and attained superior performance of 91.67% for the XCM, 88.89% for the YCM and for the ZCM 91.67%. It can be concluded that for the fMRI images, the X_axis and Z_axis views can provide more useful information than the Y_axis view.

References:

- [1] G. H. Glover, "Overview of functional magnetic resonance imaging", *Neurosurg. Clin. N. Am.*, vol. 2, no. 22, 2011.
- [2] A. S. Stratil, I. Thome, J. Sommer, and A. Jansen K. M. Zimmermann, "Illusory face detection in pure noise images: The role of interindividual variability in fMRI activation patterns" , *PLoS One*, vol. 1, no. 14, 2019.
- [3] M. Piazza, S. Dehaene, A. Kleinschmidt, E. Eger G. Lasne, "Discriminability of numerosity-evoked fMRI activity patterns in human intra-parietal cortex reflects behavioral numerical acuity", *Cortex*, vol. 114, pp. 90–101, 2019.
- [4] R. R. O. Al-Nima, "Signal Processing and Machine Learning Techniques for Human Verification Based on Finger Textures" , *Newcastle University*, 2017.
- [5] R. R. O. Al-Nima, S. Q. Hasan, and S. Esmail, "Exploiting the Deep Learning with Fingerphotos to Recognize People," *International Journal of Advanced Science and Technology*, vol. 7, no. 29, 2020.
- [6] R. R. Omar, T. Han, S. A. Al-Sumaidae and T. Chen, "Deep Finger Texture Learning for Verifying People.," *IET Biometrics*, vol. 1, no. 8, 2018.
- [7] A. J. O. Toole, "Partially distributed representations of objects and faces in ventral temporal cortex," *Journal of Cognitive Neuroscience*, vol. 17, no. 580–590, 2005.
- [8] Y. Kamitani and F. Tong, "Decoding the visual and subjective contents of the human brain", *Nature Neuroscience*, vol. 5, no. 8, 2005.
- [9] J. D. Haynes and G. Rees, "Decoding mental states from brain activity in humans", *Nature Reviews Neuroscience*, vol. 7, no. 7, 2006.
- [10] E. B. Issa, P. Bashivan, K. Kar, K. Schmidt, J. Di-Carlo , and R. Rajalingham, "Comparing object recognition behavior in humans, monkeys, and machines," *Journal of Neuroscience*, 2018.
- [11] S. Laconte, "Support vector machines for temporal classification of block design fMRI data", *NeuroImage*, vol. 2, no. 26, 2005.
- [12] D. R. Hardoon, "Unsupervised analysis of fMRI data using kernel canonical correlation", *Trends in Cognitive Sciences*, vol. 4, no. 37, 2008.
- [13] T. M. Mitchell, "Learning to decode cognitive states from brain images", *Machine Learning*, vol. 2, no. 57, 2004.
- [14] M. George, "The Visual Cortex", *Life Sciences*, 2017.
- [15] Y. Goldshmit, and J. A. Bourne C. E. Warner, "Retinal Afferents Synapse with Relay Cells Targeting the Middle Temporal Area in the Pulvinar and Lateral Geniculate Nucle" , *Neuroanatomy*, 2010.
- [16] Z. Z. Htike and N. K. A. Rashid] N. F. M. Suhaimi, "Classification of fMRI data using deep learning approach", *ARPN Journal of Engineering and Applied Sciences*, 2015.
- [17] K. Buza and Z. Vidnyánszky R. J. Meszlényi, "Resting State fMRI Functional Connectivity-Based Classification Using a Convolutional Neural Network Architecture", *journals neuroinformatics*, 2017.
- [18] Z. Wei, Y. Zhou, G. Li, X. Zhang and W. Han D. Wen, "Deep Learning Methods to Process fMRI Data and Their Application in the Diagnosis of Cognitive Impairment", *journals neuroinformatics*, 2018.
- [19] A. Insabato, A. Sanja, S. Kühn, D. Mantini, G. Deco, M. Gilson V. Pallares, "Extracting orthogonal subject- and condition-specific signatures from fMRI data using whole-brain effective connectivity", *NeuroImage*, 2018.
- [20] R. VanRullen and L. Reddy, "Reconstructing faces from fMRI patterns using deep generative neural networks", *Commun. Biol.*, vol. 2, no. 1, 2019.
- [21] M. Behroozi, M. R . Daliri, and H. Boyaci, "Statistical analysis methods for the fMRI data. ," *Basic and Clinical Neuroscience*, vol. 2, no. 4, 2011.
- [22] M. A. Lindquist, J. M. Loh, and Y. R. Yue, "Adaptive spatial smoothing of fMRI images", *Statistics and its Interface*, vol.

- 1, no. 3, 2010.
- [23] S. Rachakonda, E. Egolf, N. Correa, and V. Calhoun, "Group ICA of fMRI toolbox (GIFT) manual," *Dostupnez*, 2011.
- [24] I. Piotta, "Application of Spatial and Temporal ICA on Resting State fMRI Data to Remove Motion-related Noise," *Master thesis in Master's Level Degree in Biomedical Engineering, Università degli Studi di Padova*, 2019.
- [25] C. Porcaro, M. T. Medaglia, N. Ja. Thai, S. Seri, P. Rotshtein, and F. Tecchio, "Contradictory Reasoning Network: An EEG and fMRI", *PloS one*, vol. 3, no. 9, 2014.
- [26] M. T. Medaglia, F. Tecchio, S. Seri, G. Lorenzo, P. M. Rossini, and C. Porcaro, "Contradiction in Universal and Particular Reasoning", *Human brain mapping*, vol. 12, no. 30, 2009.
- [27] P. Khaire, P. Kumar and J. Imran, "Combining CNN streams of RGB-D and Skeletal Data for Human Activity Recognition", *Pattern Recognition Letters*, 2018.
- [28] M. M. Abuqadumah, M. A. Ali, and R. R. Al-Nima, "Personal Authentication Application Using Deep Learning Neural Network", in *16th IEEE International Colloquium on Signal Processing & its Applications (CSPA)*, Langkawi, Malaysia, 2020.
- [29] C. L. Huang, and C. Y. Tsai, "A hybrid SOFM-SVR with a filter-based feature selection for stock market forecasting," *Expert Systems with Applications*, vol. 2, no. 36, 2009.
- [30] J. Brownlee, "A Gentle Introduction to Padding and Stride for Convolutional Neural Networks", 2019.
- [31] A. Khan, A. Sohail, U. Zahoor, and A. S. Qureshi, "A survey of the recent architectures of deep convolutional neural networks," *Artificial Intelligence Review*, 2019.
- [32] Q. Zhao, S. Lyu, B. Zhang and W. Feng, "Multiactivation Pooling Method in Convolutional Neural Networks for Image Recognition", *Wireless Communications and Mobile Computing*, 2018.
- [33] Ifu Aniemeka. (2017) A Friendly Introduction to Convolutional Neural Networks. [Online]. <https://hashrocket.com>
- [34] F. Ahmed, R. Girshick, L. Zitnick, and D. Batra, and M. Cogswell, "Reducing overfitting in deep networks by decorrelating representations", *arXiv preprint arXiv:1511.06068*, 2015.
- [35] C. Couprie, L. Najman, Y. LeCun, and C. Farabet, "Learning hierarchical features for scene labeling", *IEEE transactions on pattern analysis and machine intelligence*, vol. 8, no. 35, 2012.
- [36] Y. LeCun, Y. Bengio, and G. Hinton, "Deep learning", *nature*, vol. 521, no. 7553, 2015.
- [37] Q. Guan, Y. Wang, B. Ping, D. Li, J. Du, Y. Qin, and J. Xiang, "Deep convolutional neural network VGG-16 model for differential diagnosing of papillary thyroid carcinomas in cytological images: a pilot stud," *Journal of Cancer*, vol. 10, no. 4876, 2019.
- [38] A. Krizhevsky, I. Sutskever, and G. E. Hinton, "Imagenet Classification With Deep Convolutional Nural Network", *Proceedings of the Advances in Neural Information Processing Systems*, 2012.
- [39] R. R. Omar, T. Han, S. A. Al-Sumaidae and T. Chen, "Deep Finger Texture Learning for Verifying People.," *IET Biometrics*, vol. 1, no. 8, 2018.
- [40] N. Hema Rajini, "Brain Tumor Image Classification and Grading Using Convolutional Neural Network and Particle Swarm Optimization Algorithm", *International Journal of Engineering and Advanced Technology (IJEAT)*, vol. 3, no. 8, 2019.
- [41] A. Ari and D. Hanbay, "Deep Learning Based Brain Tumor Classification and Detection System", *Turkish Journal of Electrical Engineering & Computer Sciences*, 2018.
- [42] A. S. Sufian and P. D. Farhana, "Advancements in Image Classification Using Convolutional Neural Network", *Computational Intelligence and Communication Networks, IEEE Xplore*, 2018.
- [43] S. Kerem. "Detection and Classification of Brain Tumours from MRI Images Using Faster R-CNN", *Preliminary communication*, vol. 4, no. 13, 2019.
- [44] G. Karimi and M. K. A. Adineh-vand, "A Hierarchical Convolutional Neural Network Architecture for Brain Tumor Segmentation in 3D Brain Magnetic Resonance Imaging", *Multidisciplinary Cancer Investigation*, vol. 1, no. 4, 2020.
- [45] R. R. AL-Nima, M. T. Al-Kaltakchi, S. A. Al-Sumaidae, S. S. Dlay, W. L. Woo, T. Han, and J. A. Chambers, "Personal verification based on multi-spectral finger texture lighting images", *IET Signal Processing*, vol. 9, no. 12, 2018.
- [46] R. R. Al-Nima, S. S. Dlay, W. L. Woo, "A new approach to predicting physical biometrics from behavioural biometrics", *International Journal of Computer, Information, Systems and Control Engineering*, vol. 8, no. 11, 2014.
- [47] R. R. O. Al-Nima, S. S. Dlay, W. L. Woo, and J. A. Chambers, "Efficient Finger Segmentation Robust to Hand Alignment in Imaging with Application to Human Verification", *5th IEEE International Workshop on Biometrics and Forensics (IWBF)*, 2017.
- [48] R. R. O. Al-Nima, "Design a biometric identification system based on the fusion of hand geometry and backhand patterns",

Iraqi Journal of Statistical Science, 2010.

- [49] M. A. Abdullah, R. R. Al-Nima, S. S. Dlay, W. L. Woo, and J. A. Chambers, J. A., "Cross-spectral Iris Matching for Surveillance Applications," *Springer, Surveillance in Action Technologies for Civilian, Military and Cyber Surveillance, Chapt5*, 2018.
- [50] R. R. O. Al-Nima, "Human authentication with earprint for secure telephone system", *Iraqi Journal of Computers, Communications, Control and Systems Engineering IJCCCE*, vol. 2, no. 12, 2012.
- [51] F. H. Abdulraheem. M. Y. Al-Ridha, and R. R. O. Al-Nima, "Using Hand-Dorsal Images to Reproduce Face Images by Applying Back propagation and Cascade-Forward Neural Networks", *2nd International Conference on Electrical, Communication, Computer, Power and Control Engineering (ICECCPCE19)*, 2019.
- [52] R. R. O. Al-Nima, H. N. Abdullah, T. Han and J. A. Chambers, M. T. Al-Kaltakchi, "Finger texture verification systems based on multiple spectrum lighting sensors with four fusion levels", *Iraqi Journal of Information & Communications Technology*, vol. 1, no. 3, 2018.
- [53] M. S. Majeed, R. R. O. Al-Nima and M. R. Khalil, "Personal identification with iris patterns", *AL-Rafidain Journal of Computer Sciences and Mathematics, College of Computer Sciences and Math / University of Mosul / Iraq*, vol. 1, no. 6, 2009.
- [54] R. R. Omar Al-Nima, M. Y. Al-Ridha and F. H. Abdulraheem, "Regenerating face images from multi-spectral palm images using multiple fusion methods", *TELKOMNIKA*, vol. 6, no. 17, 2019.
- [55] R. R. O. Al-Nima, N. A. Al-Obaidy and L. A. Al-Hbeti, "Segmenting Finger Inner Surface for the Purpose of Human Recognition", *2nd International Conference on Engineering Technology and its Applications (ICETA), IEEE*, 2019.
- [56] T. Han, T. Chen, R. R. O. Al-Nima "Road Tracking Using Deep Reinforcement Learning for Self-driving Car Applications", In: R. Burduk, M. Kurzynski and M. Wozniak (eds)", *Progress in Computer Recognition Systems, Progress in Computer Recognition Systems, CORES 2019, Advances in Intelligent Systems and Computing, Springer, Cham*, 2020.
- [57] R. R. O. Al-Nima and S. Kasim, "Picture Recognition by Using Linear Associative Memory Neural Network", *Tikrit Journal of Pure Science*, vol. 3, no. 13, 2008.
- [58] A. Hamed, L. H. Albak, and R. R. O. Al-Nima, "Design Security System based on Arduino", *TEST Engineering & Management, The Mattingley Publishing Co., Inc*, vol. 82, no. pp. 3341-3346, 2020.
- [59] L. H. Albak, A. H. S. Hamdany and R. R. O. Al-Nima, "Wireless Waiter Robot", *TEST Engineering & Management, The Mattingley Publishing Co., Inc*, vol. 81, no. pp. 2486-2494, November-December 2019.
- [60] R. R. Al-Nima, T. Han, T. Chen, S. Dlay , and J. Chambers, "Finger Texture Biometric Characteristic: a Survey" , *arXiv preprint arXiv*, 2020.
- [61] M. Y. Al-Ridha, R. R. O. Al-Nima, and A. S. Anaz, "Adaptive Neuro-Fuzzy Inference System for Controlling a Steam Valve," *IEEE 9th International Conference on System Engineering and Technology (ICSET)* , Shah Alam, Malaysia 2019.

